Removal of methylene blue from aqueous solutions by biochar prepared from the pyrolysis of mixed municipal discarded material

John Hoslett[1], *Heba* Ghazal[2], *Nour Mohamad*[1], and *Hussam* Jouhara[1,*]

[1]Brunel University London, College of Engineering, Design and Physical Sciences, Kingston Lane, Uxbridge UB8 3PH, United Kingdom

[2]Kingston University, School of Pharmacy and Chemistry, Kingston Upon Thames KT1 2EE, United Kingdom

[*]Corresponding Author: *hussam.jouhara@brunel.ac.uk*

List of Figures

Abstract

This paper investigates the adsorption of organic compounds in aqueous solution to biochar adsorbent, using methylene blue as an indicator for adsorption. Biochar was produced by the pyrolysis of mixed municipal discarded material in an innovative heat pipe reactor, the pyrolysis temperature was held at 300^{o}C for 12h. Biochar produced under these conditions was found to have oxygen containing functional groups that are beneficial to the adsorption of methylene blue as well as graphitic structures suggesting potential sites for π-π interactions with methylene blue. Methylene Blue followed the pseudo second order kinetic model with higher R^2 values than both the pseudo first order kinetic and intraparticle diffusion models. The adsorption also closely fit the Langmuir isotherm rather than the Freundlich model, suggesting monolayer adsorption rather than multilayer adsorption. Maximum adsorption capacity was observed at 7.2mg/g for initial concentration of 100mg/l Methylene blue in aqueous solution. The amount of Methylene blue adsorbed increased with increasing initial concentration as expected. The adsorption mechanisms are likely π-π interactions between methylene blue and the graphitic structures in the biochar which are shown to be present in Raman spectroscopy, as well as electrostatic attraction and ionic bonding between negatively charged surface sites on the char and the positive charge on the dissolved methylene blue molecules. The results show that biochar obtained from mixed waste could be employed as a low-cost and effective tool in water treatment for the removal of basic dyes and potentially other organic impurities.

Keywords

Pyrolysis, methylene blue, biochar, Mixed Municipal Discarded Material

1. Introduction

Holistic solutions for water treatment are required globally, especially in remote areas where centralised supply systems are not immediately feasible. Additionally, there is a pressing demand for sustainable waste management procedures that treat waste as a resource, rather than a by-product (Jouhara et al., 2017). These two issues often combine with disastrous effects, especially in developing communities where proper waste management practises are not adopted. This leads to the introduction of contaminants to water supplies. Waterborne contaminants introduced to water by poor waste management include heavy metals (Chowdhury et al., 2016), pesticides (Sun et al., 2019) pharmaceutical products (Branchet et al., 2019), and harmful poly-aromatic hydrocarbons (Petrovic et al., 2018). These are removed in developed nations using systems that incorporate a variation of advanced and simple filtration and separation processes (Hoslett et al., 2018). These systems for whatever reason, may not be attainable in a developing world setting, thus more simply operated systems are used to procure clean drinking water.

The removal of organic compounds from drinking water is important as trace levels of some organic contaminants may result in harmful effects on human health and the environment. Sources of organic pollution include pesticides from agricultural practices (Graf et al., 2019), industrial waste and wastewater from plastic and textile industries (He et al., 2018), and pharmaceutical/personal care products (Quesada et al., 2019) to name a few. Contamination with pharmaceuticals is a significant issue as these often contain biologically active components which lead to detrimental effects on both humans and the environment. One example of harm caused by the presence of pharmaceutical products in water is the

emergence of antibiotic resistant bacteria due to the overuse of antibiotics (Huang et al., 2019), improper disposal of antibiotics (Singh et al., 2019), or incomplete removal of antibiotics in water treatment plants (Sanganyado and Gwenzi, 2019). Another way in which organic compounds interact with the biosphere is as endocrine disruptors (US, 2019) resulting in birth defects in living organisms. Some organic compounds are not fully removed by conventional water treatment techniques and more advanced procedures are often adopted in developed nations to remove these trace organics from water (Bai and Acharya, 2019). These methods include advanced oxidation procedures namely; ozonation, UV irradiation and photo-catalysis, and other procedures such as forward osmosis (Lee et al., 2019). These processes however are technically complicated and require well trained personnel. In addition sufficient infrastructure is required for their operation, therefore these processes may not be well suited in the removal of organic pollutants from water in developing nations (Hoslett et al., 2018; Mac Mahon and Gill, 2018).

Slow sand filters are an example of an easily operated water treatment method which is used in the developing world due to its simplicity of design, construction and operation (Lee and Oki, 2013). However, this method does not significantly remove heavy metals and other toxic materials such as pesticides and pharmaceuticals from solution without modification (Manawi et al., 2018; Tizaoui et al., 2012). A method of removing such pollutants from water is through the use of solid adsorbents; this is considered an ideal technology due to its efficacy, low cost and simple operation (Gwenzi et al., 2017). Biochar adsorbents can be produced by the pyrolysis of different carbonaceous precursor materials such as sea weed, paper pulp/sludge, sugarcane bagasse, and mixed municipal discarded material (MMDM) (Ahmed et al., 2019; Chaukura et al., 2017; Lyu et al., 2018; Sumalinog et al., 2018). Studies evaluated the sorptive capacities of biochar concerning various pollutants including toxic

heavy metals such as copper, lead, cadmium (Hoslett et al., 2019; Rechberger et al., 2019; Trakal et al., 2016), metalloids such as arsenic (Wongrod et al., 2019), and both biological and non-biological organic pollutants (Ren et al., 2018; Sasidharan et al., 2016; Zhang et al., 2017). Many of these studies display the positive characteristics of char for varied contaminant removal/sorption from aqueous solutions. This material is inexpensive as it can be produced from MMDM feedstock that has little value prior to pyrolysis. It is also easy to produce in comparison to the technologically advanced water filtration methods already mentioned which require specialist knowledge and training to produce and maintain (Yaashikaa et al., 2019).

Different feedstocks can result in biochars that possess different physical and chemical properties (S. Li et al., 2019). The differing characteristics between biochars cause varying adsorption behaviours between different feedstocks. Greater negative charge can result in greater electrostatic attraction of positively charged pollutants (Tan et al., 2019) and vice versa. Increased amounts of oxygen containing functional groups result in greater complexing and/or intermolecular interactions with contaminants (Fan et al., 2018), complexation being particularly important in the removal of metals. Increased aromatic groups in the biochar can result in π-π interactions with aromatic groups in organic pollutants (Ahmed et al., 2018). Surface area is typically found to have a great impact on the adsorption of organic molecules. The previous list of biochar characteristics and the respective adsorption mechanisms they influence is not exhaustive, biochar is a highly complex medium. One way in which current literature mitigates the complexity of biochar is by using specific feedstock material (Mohammed et al., 2018; Parsa et al., 2019; Yazdani et al., 2019; Zhang et al., 2020). This makes the chemical and physical characteristics more homogenous throughout a batch of biochar produced at known pyrolysis conditions. This approach can be beneficial to industries

and areas that produce consistent types of waste materials; it is however not necessarily the best approach concerning MMDM where energy intensive, costly and technologically advanced processes are required to separate MMDM into specific feedstocks (Gundupalli et al., 2017; Meira de Sousa Dutra et al., 2018). In less developed areas where implementing a technically advanced sorting procedure is not sustainable, pyrolysis could present a possible solution to the management of MMDM, as well as the source of a possible adsorbent for water treatment.

One of the main problems with pyrolysis is that toxic compounds such as dioxins and polyaromatic hydrocarbons (PAHs) can be produced (Zhou et al., 2015). PAHs and Dioxins are poorly soluble in water however they have been found on fine dust particles which could be suspended in water (Minomo et al., 2018; Vandermarken et al., 2018). This is problematic when using biochar for water treatment since leached PAHs and dioxins are hazardous and lead to health complications in humans (Chen et al., 2019).

It has been found that lesser amounts of PAHs occur in biochar produced at lower temperature compared to biochar produced at higher temperature (Chen et al., 2019). Some studies have found that PAHs are more abundant in materials produced by fast pyrolysis and gasification than slow pyrolysis (Hale et al., 2012). Other factors such as feedstock type also play a large role in PAH production (Buss et al., 2016). One way of reducing PAH content in pyrolysis materials is to pyrolyze at very high temperatures (>700^{o}C), this leads to the vaporisation of PAHs in biochar and has the added benefit of producing biochar with increased surface areas (Czajczyńska et al., 2017). However, decreased amounts of biochar is produced at these high temperatures compared with low temperatures (Li et al., 2011; Yang et al., 2018). In addition these high pyrolysis temperatures result in the loss of surface functional groups that can be highly beneficial for adsorption (Tang et al., 2019). Reducing

PAHs and dioxins can also be achieved through the utilisation of lower pyrolysis temperatures and slow pyrolysis rather than fast pyrolysis. PAHs and dioxins are formed in significantly lesser amounts under these conditions (Hu et al., 2019; Zhou et al., 2016). Furthermore, avoiding the use of certain feedstocks such as chlorine containing plastics, or copper containing materials can reduce the amounts of dioxins produced by the incomplete dehydrochlorination and de novo synthesis pathways respectively (Huang and Buekens, 1995; Zhou et al., 2016). PAHs can also be reduced through avoiding the use of certain feedstocks, mainly plastics (L. Li et al., 2019; Zhou et al., 2015). Moreover, the production of biochar adsorbents using a heat pipe based reactor has not to the knowledge of the authors been conducted in any current literature.

Consequently, this study was conducted to investigate the use of biochar derived from MMDM not including plastic, using low temperature, slow pyrolysis produced in a heat pipe reactor for the removal of organic pollution from water using MB as an indicator pollutant. MB is an organic dye that has a wide range of applications; medical, textile and in printing industries (Molina Higgins et al., 2019). MB was therefore selected as an indicator of MMDM biochar adsorption performance for this study.

2. Materials and Methods

2.1 Materials

Methylene Blue Hydrate, 0.5M Titripur sulfuric acid and 0.5M Titripur sodium hydroxide were obtained from Sigma Aldrich. 0.45μm Nalgene syringe filters (Thermofisher) were obtained from Fisher Scientific.

2.2 Biochar production

Biochar was obtained from MMDM pyrolysed in a heat pipe reactor seen in **Fig. 1**. Pyrolysis temperature was maintained at 300^{o}C for a retention time of 12h. The MMDM used in this

study consisted of paper, cardboard, food scraps and garden waste. Paper and cardboard char were described as paper/cardboard char, and food scraps/garden waste were described as food/garden char. Previous experiments by the author found plastic to be unfavourable for adsorption as the pyrolysis temperatures used were not high enough to result in the full pyrolysis of plastic discarded materials (Hoslett et al., 2019). Additionally, developing countries produce higher levels of organic discarded materials than discarded plastics (Kaza et al., 2018), these can include food scraps and agricultural waste which are similar to garden trimmings and food scraps.

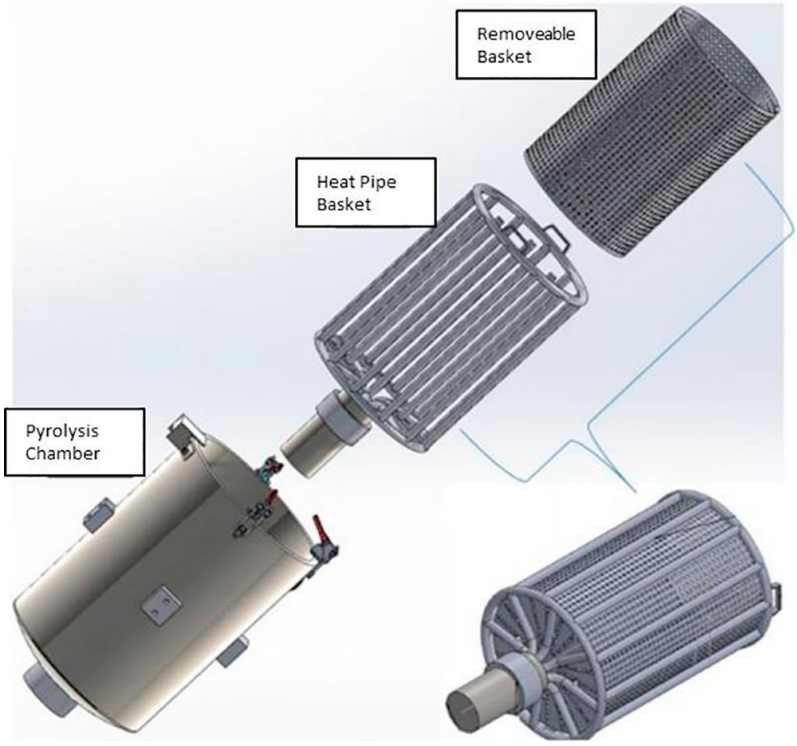

Fig. 1. Schematic drawing of pyrolysis reactor used in this study (Jouhara et al., 2018).

2.3 Biochar characterisation

The biochar was characterised prior to adsorption experiments using four different techniques: Scanning Electron Microscopy (SEM), Energy Dispersive X-ray Analysis (EDAX), Fourier Transmission Infra-Red spectroscopy (FTIR), and Raman spectroscopy. SEM was used to explore the surface morphology of the biochar, with two different samples of

paper/cardboard and food/garden biochar used to illustrate the variation in biochar characteristics between two feedstocks. EDAX was used to determine the elemental composition of the biochar illustrating the difference between different feedstocks using two separate samples of food/garden char and paper/cardboard char. FTIR was used to observe the different functional groups present within the mixed char. Raman spectroscopy was used to investigate the crystalline structure of the mixed char, more specifically it was used to reveal the graphitic and amorphous structures present in the char.

2.4 UV-Vis Spectrophotometry

UV-Vis spectrophotometry was used to determine concentration of MB before and after adsorption. A wavelength of 664nm was analysed as this was found to be the maximum absorption peak for MB in solution. MB solutions between concentrations of 0-3 mg/l were used for a calibration curve, this was the linear range for UV-Vis absorbance of MB solution. Sample solutions were diluted to fall within this concentration range for analysis.

2.5 Adsorption Kinetic experiments

A 1000mg/l stock solution of MB was prepared by dissolving 1.288g of Methylene blue hydrate in 1L of water. This solution was diluted to produce initial concentrations of 10, 25, 50, 75 and 100mg/l MB solution. The pH of the solutions was adjusted to pH 5 using 0.5M sodium hydroxide and 0.5M sulphuric acid. Adsorption times of 5, 10, 20, 30, 60, 180, 270 and 360 minutes were used for these experiments. A maximum contact time of 6h was selected due to the focus of this study on biochar as a potential filtration media. 5ml samples were collected and passed through 0.45μm Nalgene syringe filters (Thermofisher) prior to UV-Vis analysis. Analysis was conducted in triplicate.

The kinetic models selected for analysis were the pseudo second order, pseudo first order and intraparticle diffusion model shown in equations (3), (4), and (5) respectively. Q_t is the

adsorption amount (mg/g) at a given time (t) is the duration of experiment (mins), K_2 is the PSO constant (g mg^{-1} min^{-1}), Q_e is the adsorption amount at the equilibrium concentration (mg/g), K_1 is the PFO constant (min^{-1}), k_i is the intraparticle diffusion rate constant (mg g^{-1} min^{-1}). The models were analysed using non-linear regression to compare with the experimental data.

$$Q_t = \frac{k_2 * {Q_e}^2 * t}{1 + k_2 * Q_e * t} \quad (3)$$

$$Q_t = Q_e * (1 - e^{-k_1 * t}) \quad (4)$$

$$Q_t = k_i * t^{1/2} + C \quad (5)$$

2.6 Adsorption Isotherm experiments

To investigate isothermal behaviour of MB sorption to biochar, initial concentrations between 10 and 100mg/l MB were used to produce different equilibrium concentrations at pH 5, stirring speed 360rpm, temperature 30°C. Equations (6) and (7) (8) show Langmuir, Freundlich and Sips isothermal models respectively. The data from isothermal experiments was analysed using non-linear regression models. Where C_e is the equilibrium concentration (mg/l), Q_e is the adsorption of MB at equilibrium (mg/g), K_L is the Langmuir constant (l/mg), Q_m is the maximum adsorption capacity (mg/g), K_f and n are both Freundlich constants, K_S is the Sips equilibrium Constant and N is the Sips model exponent.

$$Qe = \frac{K_L * Q_m * C_e}{1 + K_L * C_e} \quad (6)$$

$$Q_e = K_f * {C_e}^{1/n} \quad (7)$$

$$Q_e = \frac{Q_m * (K_S * C_e)^N}{(K_S * C_e)^N + 1} \quad (8)$$ (Tong et al., 2018)

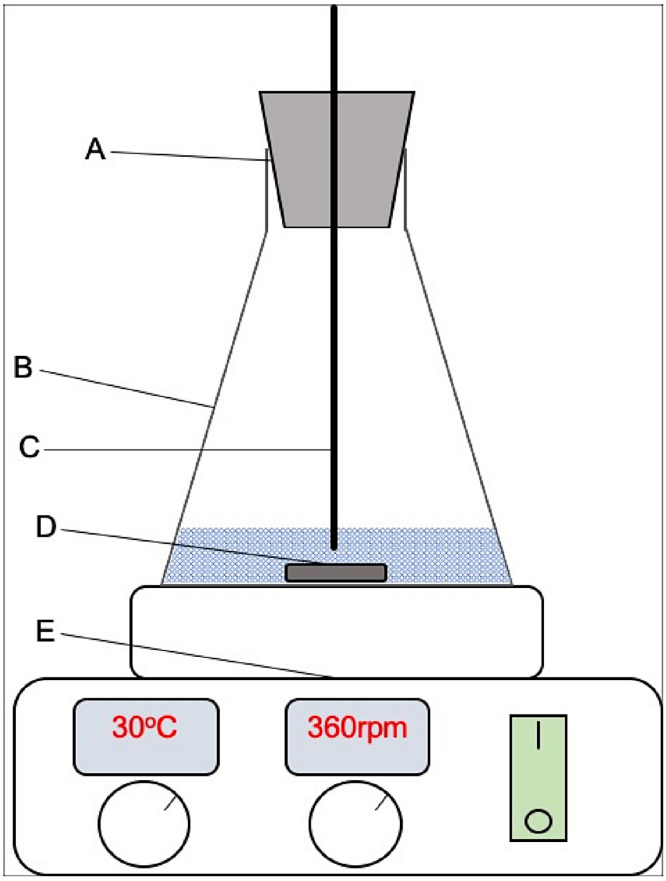

Fig. 2. Experimental set up for MB Kinetic and Isothermal experiments (A) shows the rubber bung in the neck of the conical flask (B), with the temperature control probe (C) inserted through a small hole in the bung, (D) shows the magnetic stirring pill and (E) shows the magnetic stirring plate itself (Hoslett et al., 2019).

2.7 Statistical analysis and modelling

Equation (1) shows the adsorption of MB after a given time, with (2) showing the adsorption of MB at equilibrium concentration. (3), (4) and (5) show the non-linear equations of the pseudo second order (PSO) and pseudo first order (PFO) kinetic models and intraparticle diffusion model respectively, where Q_t is the adsorbed amount at a given time (mg/g), V is the volume of solution (l), C_i is the initial MB concentration (mg/l), C_t is the MB concentration at a given time (mg/l), C_e is the concentration at equilibrium (mg/l) , m is the mass of adsorbent used (g),

$$Q_t = \frac{V*(C_i - C_t)}{m} \quad (1)$$

$$Q_e = \frac{V*(C_i - C_e)}{m} \quad (2)$$

All experiments were carried out in duplicate with the average values analysed.

2.8 Molecular orbital modelling

Molecular orbital modelling of MB molecules was carried out in order to determine whether π-π interactions are possible between MB molecules and biochar surface. This was conducted using Avogadro molecular editing and visualisation software. Avogadro was used to generate the input for the Orca quantum chemistry program. The geometry optimisation procedure was conducted using density functional theory in order to develop visualisations of the molecular orbital shape. The orbital shape revealed the nature of the molecular orbitals.

3 Results

3.1 Biochar characterisation

SEM analysis was conducted to study the surface morphology of biochar produced from the pyrolysis of MMDM. The MMDM used in this study was separated into food/garden and paper/cardboard feedstocks for characterisation before being mixed for adsorption experiments. The SEM for these can be seen in **Fig. 3** A and B, respectively. The corresponding EDAX analysis for the food/garden biochar paper/cardboard biochar are displayed in **Fig. 3** A2 and B2, respectively. These figures show the elemental content and composition of the two full areas analysed and expresses these in terms of the atomic percentage.

The SEM image of biochar produced from paper/cardboard appears to have a lattice-like structure distinctive of biochar derived from paper (Hoslett et al., 2019). Meanwhile the SEM image of biochar produced from food/garden material appears to have a heterogenous surface morphology with pores of varying sizes. This heterogeneity of the food/garden biochar surface structure and the lattice structure of the paper/carboard biochar imply that a greater surface area is available for adsorption food/garden material than paper/cardboard. These SEM images further demonstrate how the use of different feedstock alters the

structure and surface morphology of the biochar produced; this in turn determines its adsorption properties.

An atomic percentage of approximately 70% carbon proves that the composition of both biochars is dominated by carbon structures, with this percentage in the food/garden biochar being slightly higher than in the paper/cardboard biochar. This could be due to paper being primarily composed of cellulose; which require temperatures that exceed the 300^{o}C used to pyrolyze the municipal solid waste in these experiments (Sophonrat et al., 2018).

The second and third most dominant elements in both biochars are oxygen and calcium with slightly higher atomic percentages of 17.7% oxygen and 5.4% calcium found in food/garden waste and paper/cardboard biochar. The presence of calcium and oxygen in the biochar containing pyrolyzed paper is most likely due to the use of calcium carbonate in the manufacturing of paper as a filler or a coating (Devi and Saroha, 2013). The detection of certain minerals in the biochar is due to their existence in the precursor materials (Schreiter et al., 2018) except for the detected gold which is present due to the gold coating applied during sample preparation for SEM-EDAX. The elements chloride, sodium, potassium, nitrogen, aluminium and phosphorus were detected in both biochars in differing percentages.

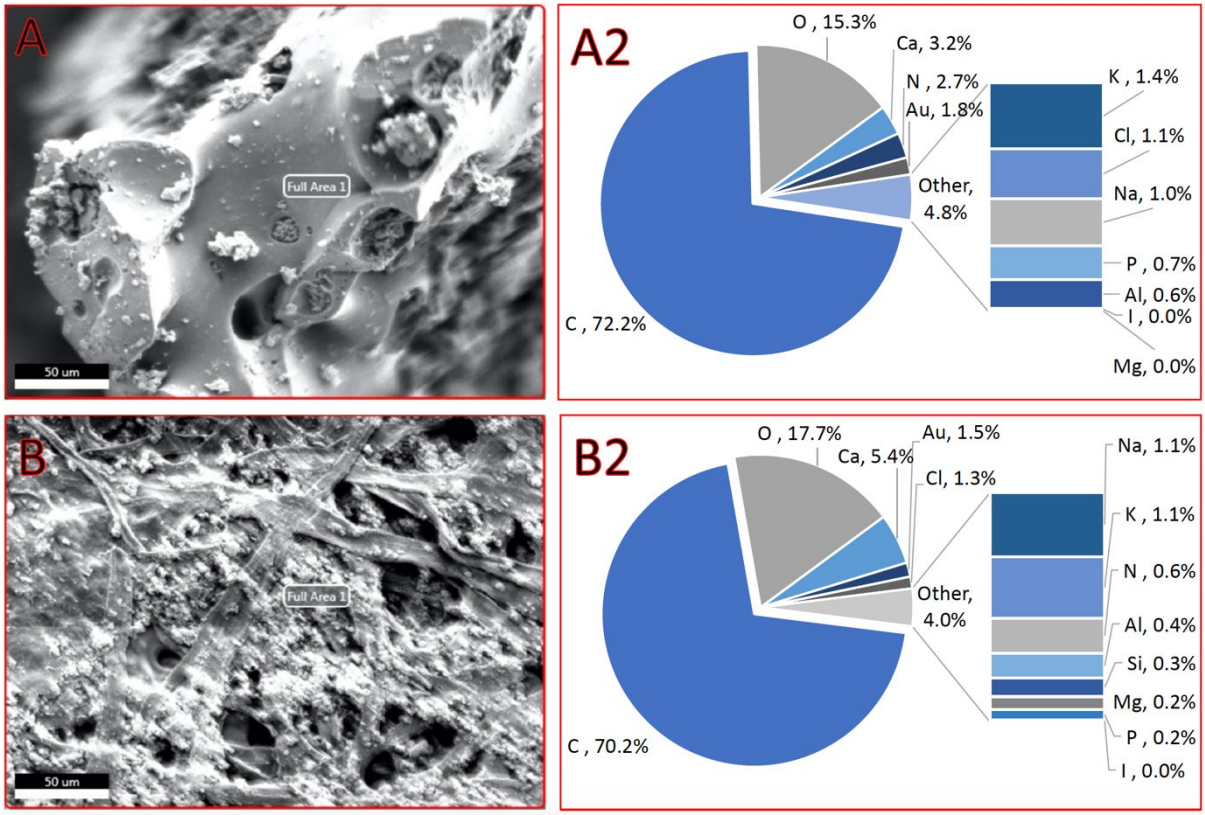

Fig. 3. SEM images of food/garden (A) and paper/cardboard (B) biochar, and EDAX results of food/garden (A2) and paper/cardboard (B2) biochar.

Fig. 4 shows the FTIR spectra for MMDM biochar. The peaks at 1416, 873 and 712 cm^{-1} are indicative of CO_3 presence in the biochar (Farges et al., 2018). Calcium carbonate is typically used in the manufacture of paper, and is also present in biological materials such as manure and grasses (Seo et al., 2017; Van Poucke et al., 2019) with 666cm^{-1} indicating the presence of CH_2 groups on the biochar surface (Litescu et al., 2012). The less intense peak between 3500-3000 cm^{-1} denotes the presence of O-H groups within the biochar, with the presence of phenolic O-H groups potentially masked in **Fig. 4** by the calcite peak between 1550 – 1350 cm^{-1}.

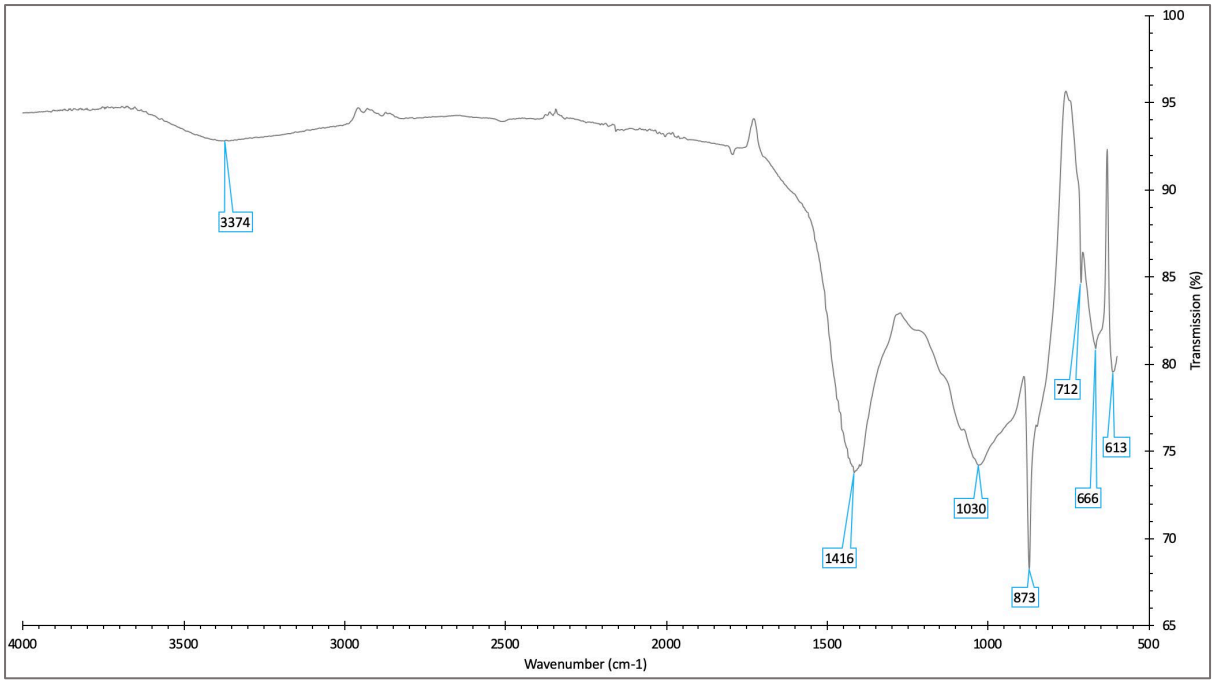

Fig. 4. FTIR results for MMDM biochar.

The results of the Raman analysis are displayed in **Fig. 5**. The two main peaks that relate to carbon structures within the biochar are observed at approximately 1600cm^{-1} and 1370cm^{-1} these indicate graphitic (G) and disordered (D) carbon structures respectively (Fuertes et al., 2010; Sheng, 2007). These two peaks indicate the presence of aromatic C-C Sp^2 hybridized bonds of benzene rings in the biochar. The G peak corresponds to an ordered graphitic lattice and is of a higher intensity than the D peak which represents the defect region of disorganised graphitic structures. This suggests there are both ideal and disordered graphitic structures in the body of the biochar, but that the biochar has a greater proportion of ordered graphitic carbons (Sheng, 2007). The sharp peak present at 1086cm^{-1} indicates the presence of calcite in the biochar (Buzgar and Ionut Apopei, 2009). The band between the D and G peaks is known as the valley section (V band), this section is indicative of amorphous carbon within the biochar (Ibn Ferjani et al., 2019). The intensity of the V band compared with the G and D peaks in this study shows that biochar produced from MMDM at 300^{o}C is a mixture of amorphous and aromatic structures.

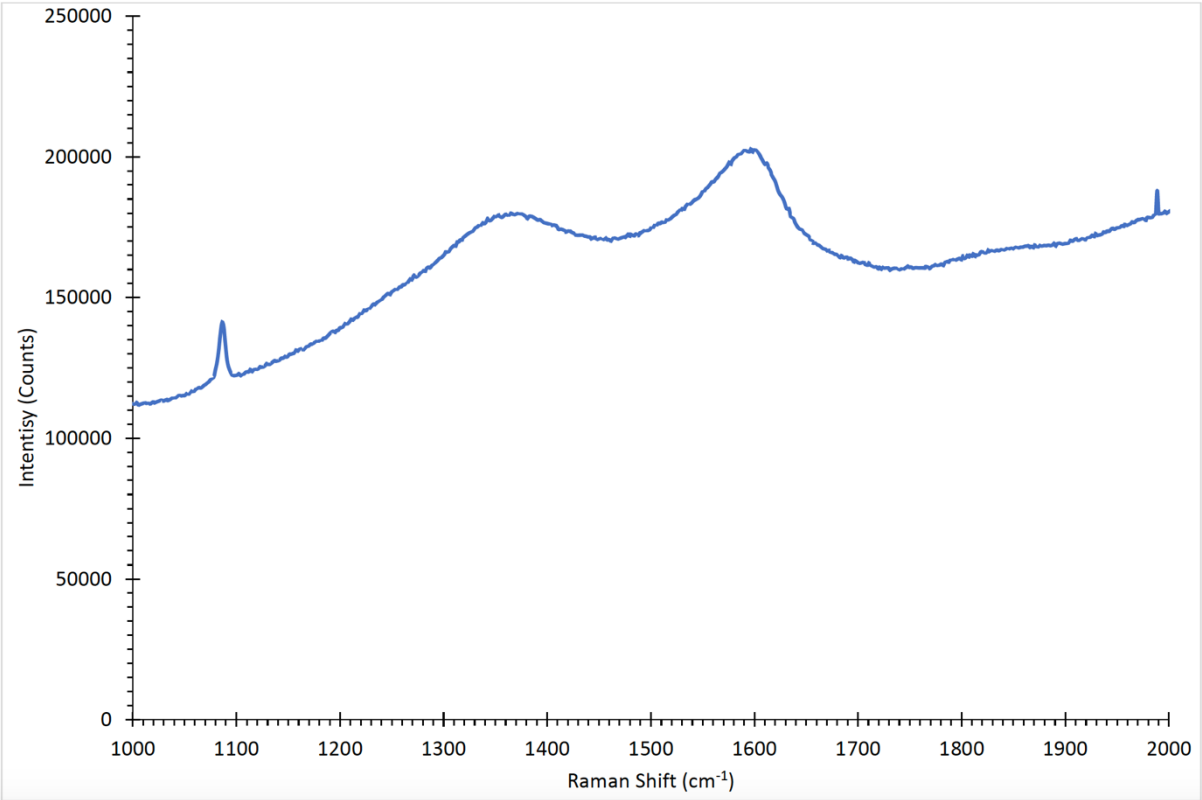

Fig. 5. Raman shift data for the MMDM biochar plotting counts against wavenumber (cm^{-1}).

3.2 Effect of adsorption time

Fig. 7 shows the kinetic data for MB adsorption to biochar, categorised by initial concentration. Model lines presented in the graph show the pseudo second order model, this model was the closest fitting kinetic model in all experiments, as demonstrated in **Table 1**. **Table 1** shows the kinetic data for experiments investigating the effect of adsorption time on the amount of MB adsorbed to the biochar. It can be seen that the kinetic model that best describes the adsorption of MB to MMDM biochar is the pseudo second order model with an R^2 value greater than both pseudo first order and intraparticle diffusion model. The pseudo second order kinetic model accounts for liquid film diffusion, surface adsorption and intra-particle diffusion processes, with the pseudo second order also stipulating that the predominant rate limiting steps are chemisorption processes (Fan et al., 2017). The reduction

of K_2 value with increasing MB concentration confirms that physisorption processes also have a limiting effect on the adsorption of MB to biochar derived from MMDM (Rehman et al., 2018).

Literature tends to focus on the pyrolysis of specific feedstock materials whereas this work focuses on the use of mixed feedstocks including garden waste, food scraps, and paper. The characterisation of different biochars in literature shows that different feedstocks pyrolyzed under similar conditions produce biochars with varying chemical and physical characteristics. This affects the adsorption properties of biochar (S. Li et al., 2019; Rajapaksha et al., 2019). The biochar precursor used in this study was thoroughly mixed. It was therefore not possible to determine the derivative feedstock proportions in any given sample of biochar. This means that the adsorption chemistry is somewhat more complex than is the case in other studies.

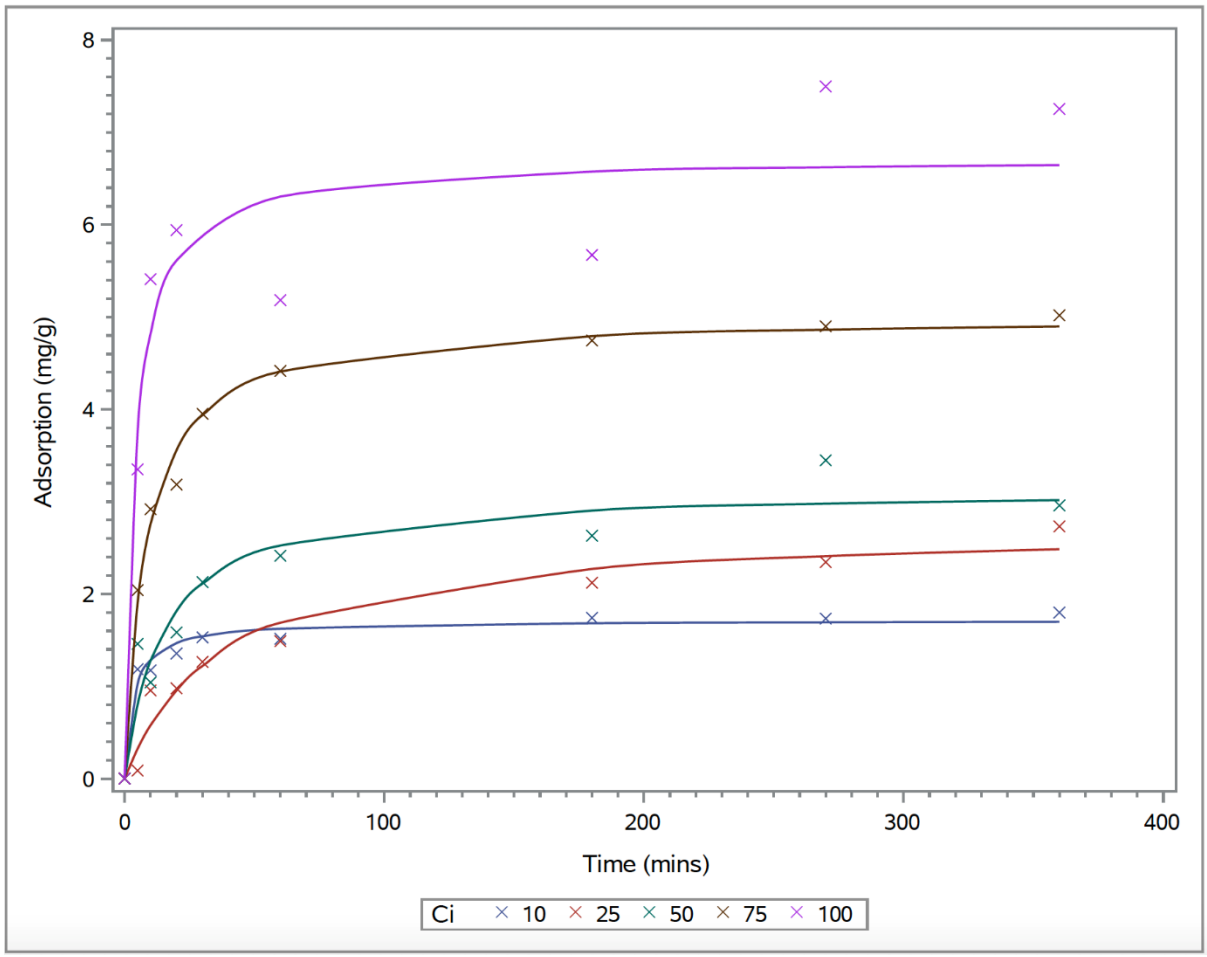

Fig. 6 – Scatter plot showing kinetic data of MB adsorption to biochar for different initial MB concentrations (Ci, mg/l) with Pseudo Second Order models shown as lines

Table 1 – Kinetic results of methylene blue adsorption to MMDM derived biochar.

Initial Conc. (mg/l)	Intraparticle diffusion model			Pseudo First Order			Pseudo Second Order		
	K_i	C_i	R^2	Q_e	K_1	R^2	Q_e	K_2	R^2
10	0.0621	0.8407	0.5689	1.615	0.1854	0.9154	1.7143	0.1733	0.9683
25	0.1366	0.2388	0.9296	2.3888	0.0231	0.9304	2.7437	0.00973	0.9547
50	0.1414	0.8335	0.8025	2.913	0.0466	0.8776	3.1385	0.0219	0.9083
75	1.8195	0.2058	0.7047	4.6873	0.0799	0.9583	5.0096	0.0245	0.9908
100	0.2647	2.8401	0.6101	6.3878	0.1615	0.8988	6.7192	0.0377	0.9055

3.3 Effect of initial Methylene Blue Concentration

Table 2 shows the isothermal data for MB experiments 10-100mg/l initial MB concentration at pH 5. The table shows that the Langmuir isotherm has an R^2 value of 0.8638. The Langmuir model accounts for monolayer adsorption whereas the Freundlich model accounts for multi-layer adsorption. Therefore, what the isothermal models show is that monolayer adsorption is the best way to describe the adsorption of MB to biochar at a time of 6h.

The performance of the MMDM biochar in this study exceeds that of paper, and pinewood derived biochar reported by Lonappan et al., 2016. However, biochars that have undergone activation processes outperform the MMDM char (S. Liu et al., 2019; Que et al., 2018). What the results and the mentioned literature suggest is that the MMDM char can be used to remove organic pollutants from water; however, the adsorption of such pollutants to non-activated MMDM char is not as favourable as is the case for different activated biochars produced in other studies. It is likely therefore that an activation process could enhance the adsorption of organic contaminants to biochar derived from MMDM however further work is needed to confirm whether this is true, and to optimise the activation procedure.

Table 2 – Isothermal models coefficients for 10-100mg/l initial MB conc. at pH 5.

Freundlich			**Langmuir**			**Sips**			
n	**K_f**	**R^2**	**Q_m**	**K_L**	**R^2**	**Q_m**	**K_{Lf}**	**N**	**R^2**
1.8746	0.6660	0.7645	365.9	0.000287	0.8638	20.2824	0.000486	0.3572	0.6752

3.4 Molecular Modelling

π electron donor-acceptor (EDA) interaction is an adsorption mechanism that involves π electrons in either the adsorbent and adsorbate, where functional groups such as amines and

methyl in either the biochar or adsorbate act as π electron acceptors (Zhao et al., 2019). These π electron acceptors are present in MB at both ends of the molecule in the R-N(CH_3)$_2$ groups. Furthermore, π-π stacking interactions can also occur between aromatic groups in both the adsorbate and adsorbents (J. Liu et al., 2019). π orbitals are shown to exist in the adsorbate by the modelling displayed in **Fig. 8**. The Raman shift characterisation data shows the presence of aromatic groups in the biochar. This shows that π interaction between MB and the MMDM biochar is possible.

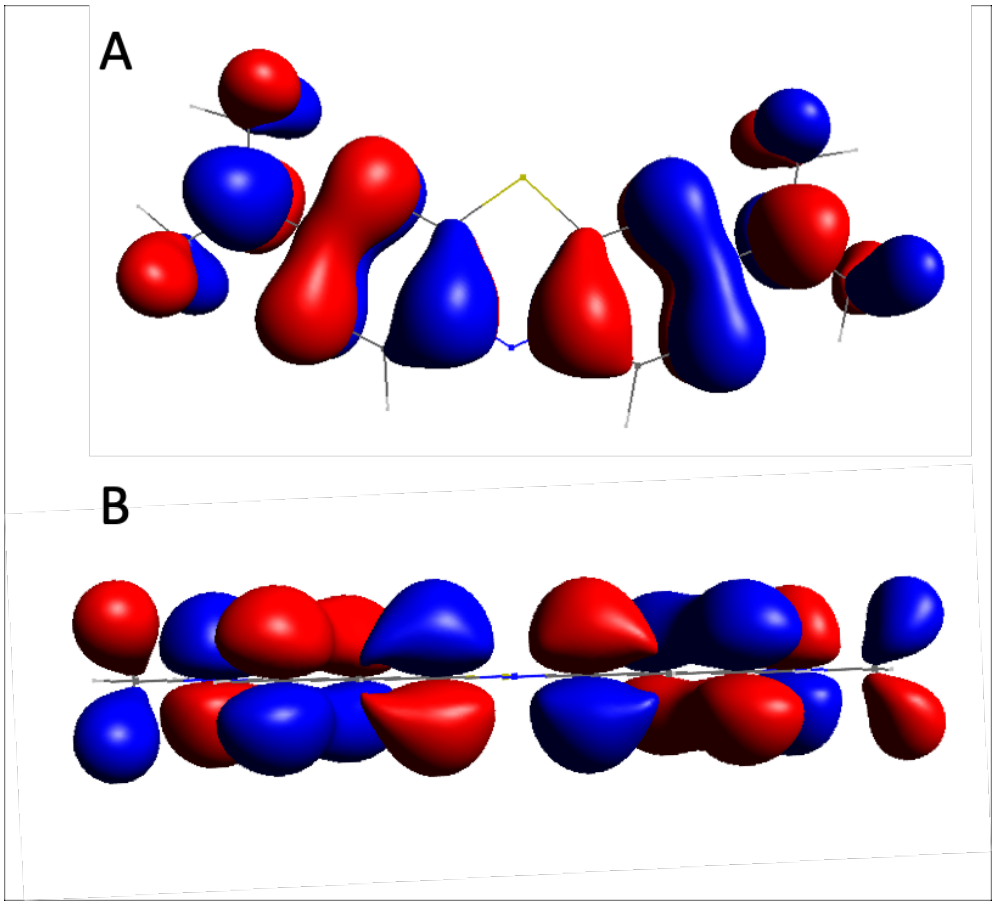

Fig. 7 – The Highest Order Molecular Orbitals (HOMO) of a Methylene Blue Molecule with (A) showing the view from above, and (B) from the side, produced using Avogadro molecular modelling software with the Orca quantum chemistry program

Fig. 9 shows the electro-static characteristics of a methylene blue molecule, with blue indicating a positive charge and red indicating negative charge. The Langmuir model fit the

actual data more closely than the Freundlich or Sips isotherm. Interactions between dissolved and absorbed MB molecules are unlikely as the Langmuir model describes monolayer adsorption (Shooto et al., 2020).

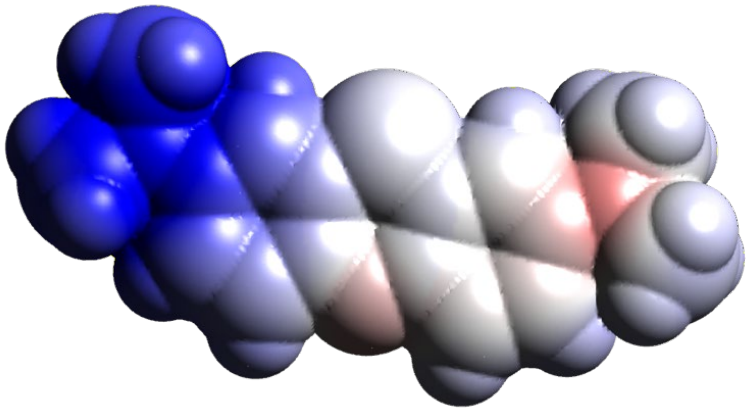

Fig. 8. Electro-static potential diagram of a methylene blue molecule

4 Discussion

4.1 Adsorption Mechanisms

The MMDM char shows a significant removal capacity of MB after 6h, despite not being activated as in other studies. This is promising for developing world applications where technically complicated activation procedures such as steam or chemical activation may not be sustainable. The sorption of MB suggests that MMDM biochar could be suited to use in the removal of small concentrations of pesticides, and pharmaceuticals in developing world applications. This MMDM biochar would also have the benefit of being produced from locally sourced biomass including domestic food scraps as well as discarded agricultural material.

The low amount of MB removed by the biochar can be explained by the pyrolysis temperature used, where pyrolysis temperatures lower than 300^{o}C can increase the adsorption of MB to biochar due to the increased amount of oxygen containing functional groups (S. Liu et al.,

2019). Increases in pyrolysis temperatures result in the volatilisation of non-carbon elements, notably hydrogen and oxygen are driven off at higher pyrolysis temperatures. This results in the loss of oxygen containing functional groups on the biochar surface. These functional groups can be important as they result in negative surface charge. Therefore, lower pyrolysis temperature can be beneficial for MB removal as the positively charged site on MB is attracted to negatively charged sites on the biochar (Zhu et al., 2018). Despite this, the data collected from this study is comparable to adsorption amounts from other similar studies concerning more specific feedstocks as seen in **Table 3**.

In addition to electrostatic interactions, π-EDA interactions between methylene blue and biochar may be benefited by the lower pyrolysis temperature used in this study. Methyl groups are attached at both ends of the MB molecule and these may interact with the π electrons present in the graphitic surfaces in the biochar that were shown to exist in the Raman spectroscopy displayed in **Fig. 5**. In addition, π-π stacking interactions are also possible between MB and biochar where π electrons also exist in the MB as shown in **Fig. 8**. π interactions tend to be enhanced by higher pyrolysis temperatures where biochar becomes more aromatic due to the higher pyrolysis temperature (Wei et al., 2019). The large amount of oxygen shown to be present in the biochar in **Fig. 3** also indicates that hydrogen bonding is possible between the surface of the biochar, and the primary amine groups at both ends of the MB molecule (S. Liu et al., 2019).

The adsorption of MB to the biochar in this study is therefore a mixture of mechanisms likely involving electrostatic interactions between the biochar and MB, π-π stacking interactions, and π-EDA interactions, and hydrogen bonding.

4.2 Comparison to other studies

The data presented in this study shows that biochar produced from MMDM can be used to remove MB from water. MB has similar structural characteristics to some pesticides and pharmaceutical compounds containing benzene rings important for π-π interactions with the biochar, polar/ionic characteristics (Paunovic et al., 2019; Zhang et al., 2019), and functional groups capable of hydrogen bonds (Suo et al., 2019). It stands to reason that the adsorption of MB in this study can be used as an indicator for MMDM biochar's capability to remove other harmful organic compounds from water. It can therefore be seen from this study that biochar produced in a heat pipe reactor from MMDM at temperatures of 300^{o}C could be used in water treatment applications to remove harmful pesticides and pharmaceutical compounds and by-products from water.

Table 3 shows the adsorption results in this study compared with other studies. What is shown is that other studies make use of higher pyrolysis temperatures, and activation procedures. The purpose of this study was to produce a biochar that could be produced quickly and easily on a large scale in a developing country for use as an adsorbent for harmful organic compounds. To that end a heat pipe reactor was used to pyrolyze the MMDM, compared to the studies mentioned which commonly purge a chamber with N_2 gas, before heating the chamber. These are also conducted on a small-scale producing around 0-50 grams of biochar using tube furnaces and the like, whereas the experimental heat pipe pyrolysis reactor used in this study produces biochar on the order of kilograms.

Table 3 also contains information on the characteristics of biochar found in other studies. These other studies that utilised higher temperatures still contained oxygen and hydrogen containing functional groups important for interaction with MB. However, the apparent amplitude of the indicative peaks in FTIR of these studies was lesser than found in this study.

Some of these studies such as Rashid et al., 2019 and Wang et al., 2018 utilised nitric acid potentially making more adsorption sites available following the removal of carbonates by this activation method. However, the feasibility of using such an activating reagent in a developing nation setting is debateable due to the expertise, training and equipment required to handle nitric acid. Furthermore, a similar study displayed in the table utilising sewage sludge and tea waste found that -C=O, -COOH, -CH, and -OH groups were potentially important for MB adsorption to biochar (Fan et al., 2016). The major benefit of the biochar used in the current study is that functional groups are not removed as the pyrolysis temperature is low in comparison to other studies where their abundance is reduced. This allows this unmodified biochar to remove MB and potentially other organic contaminants. Further modifications of this biochar could vastly improve its performance in adsorption of MB (Rashid et al., 2019).

What is also seen in the table is that these other studies use higher pHs for the adsorption of MB to biochar. This comes after identifying the pH of zero charge. The pH of zero charge is the value of pH at which the biochar has no electrical charge, typically a pH below this point means the biochar in suspension has a positive charge, and above this point a negative charge. The reason studies use high pH values is to maximise the adsorption of methylene blue to biochar. With a positive charge when dissolved, MB molecules are more strongly attracted to a biochar that has a negative charge compared to a positive charge, thus a biochar in a high pH solution will adsorb more MB than a biochar in a low pH solution. Increasing the pH of the polluted water to maximise adsorption may not always be possible in developing world applications, so it was important to investigate non-favourable conditions as well as favourable conditions already reported in literature.

Table 3 – Adsorption results from this study and other studies.

Feedstock	Pyrolysis conditions / biochar composition	Experiment duration (h)	Biochar Dosage (g/l)	Initial conc. (mg/l)	pH	Amount adsorbed (mg/g)	Source
MMDM	300°C, 12h, heat pipe / hydrogen and oxygen containing functional groups present, graphitic and disordered carbon structures present	6	5	10	5	1.798	This study
MMDM	300°C, 12h, heat pipe / hydrogen and oxygen containing functional groups present, graphitic and disordered carbon structures present	6	5	25	5	2.732	This study
MMDM	300°C, 12h, heat pipe / hydrogen and oxygen containing functional groups present, graphitic and disordered carbon structures present	6	5	50	5	2.960	This study
MMDM	300°C, 12h, heat pipe / hydrogen and oxygen containing functional groups present, graphitic and disordered carbon structures present	6	5	75	5	5.018	This study

MMDM	300°C, 12h, heat pipe / hydrogen and oxygen containing functional groups present, graphitic and disordered carbon structures present	6	5	100	5	7.254	This study
Tea waste mixed with sewage sludge	300°C, 2h / hydrogen and oxygen containing functional groups present, graphitic and disordered carbon structures present	24	Not reported	100	-	8.945	(Fan et al., 2016)
Municipal solid waste (60% paper, 25% garden waste, 15% textile)	400-500°C 15 min purge, 30 min pyrolysis / hydrogen and oxygen containing functional groups present	4	2	50	6.5	21.83	(Sumalinog et al., 2018)
Pumpkin peel	250°C 60 min pyrolysis time Activated after pyrolysis with beetroot juice at 100°C / Functional groups increased significantly following beetroot juice modification	3	0.5	50	7	80.782	(Rashid et al., 2019)

Pumpkin peel	250^{o}C 60 min pyrolysis time Activated after pyrolysis with beetroot juice at 100^{o}C / Functional groups increased significantly following beetroot juice modification	3	2	50	7	25.113	(Rashid et al., 2019)
Reeds	500^{o}C pyrolysis time 2h, activated using nitric acid, adsorption enhanced by presence of tannic acid / nitric acid removed carbonate from biochar	24	1	50	8	48.84	(Wang et al., 2018)
Eucalyptus sawdust	400^{o}C pyrolysis time 30min, / Oxygen and hydrogen containing functional groups present, but less peak heights in FTIR than this study	4	8	15	Not reported	0.957	(Sun et al., 2013)
Palm bark	400^{o}C pyrolysis time 30min, / Oxygen and hydrogen containing functional groups present, but less peak heights in FTIR than this study	4	8	15	Not reported	1.217	(Sun et al., 2013)

Anaerobic digestion residue	400^{o}C pyrolysis time 30min, / Oxygen and hydrogen containing functional groups present, but less peak heights in FTIR than this study	4	8	15	Not reported	1.694	(Sun et al., 2013)

4.3 Implications for the developing world

Producing biochar from MMDM could present a potential solution to people in developing countries for the removal of harmful organic pollutants such as pesticides and pharmaceutical products from water. The cost of such a material is low in comparison to more advanced techniques used in developed nations (Chowdhury et al., 2016). Following filtration this biochar could be further utilised for other purposes, such as a fuel or soil additive depending on the quality (Gwenzi et al., 2015; Yuan et al., 2019). This circular economy approach could therefore increase the life quality of people in rural developing areas, making their drinking water cleaner, agricultural activities more efficient and productive, as well as providing a cleaner burning fuel that poses less of a risk than traditional fuel sources (Acharya and Marhold, 2019; Gwenzi et al., 2017).

5 Conclusion

MMDM char derived from heat pipe- based pyrolysis reactor showed a strong capability for the removal of MB from aqueous solution in a short time span. This could be concluded due to the adsorption capacity of MB to biochar reaching 7.2mg/g in a concentration of 100mg/l at pH 5. It is therefore possible to see that this char could be produced for use in filter applications to remove harmful organic compounds such as pesticides and residual pharmaceuticals from surface waters in the developing world. However, more work is needed to increase the adsorption capacity of biochars derived from MMDM to make this competitive with commercial activated carbons, as well as optimising their removal of harmful organic compounds in developing countries. Nonetheless the adsorption capacity of MB onto biochar is shown to be comparable to other studies and thus it is concluded that biochar produced from MMDM at 300^{o}C could be used to remove harmful organic pollutants from water.

ACKNOWLEDGMENT

The reported work was funded by EPSRC under Grant 1956470.

6 References

Acharya, B., Marhold, K., 2019. Determinants of household energy use and fuel switching behavior in Nepal. Energy 169, 1132–1138. https://doi.org/https://doi.org/10.1016/j.energy.2018.12.109

Ahmed, M.B., Zhou, J.L., Ngo, H.H., Johir, M.A.H., Sun, L., Asadullah, M., Belhaj, D., 2018. Sorption of hydrophobic organic contaminants on functionalized biochar: Protagonist role of π-π electron-donor-acceptor interactions and hydrogen bonds. J. Hazard. Mater. 360, 270–278. https://doi.org/https://doi.org/10.1016/j.jhazmat.2018.08.005

Ahmed, M.J., Okoye, P.U., Hummadi, E.H., Hameed, B.H., 2019. High-performance porous biochar from the pyrolysis of natural and renewable seaweed (Gelidiella acerosa) and its application for the adsorption of methylene blue. Bioresour. Technol. https://doi.org/https://doi.org/10.1016/j.biortech.2019.01.054

Bai, X., Acharya, K., 2019. Removal of seven endocrine disrupting chemicals (EDCs) from municipal wastewater effluents by a freshwater green alga. Environ. Pollut. 247, 534–540. https://doi.org/https://doi.org/10.1016/j.envpol.2019.01.075

Branchet, P., Ariza Castro, N., Fenet, H., Gomez, E., Courant, F., Sebag, D., Gardon, J., Jourdan, C., Ngounou Ngatcha, B., Kengne, I., Cadot, E., Gonzalez, C., 2019. Anthropic impacts on Sub-Saharan urban water resources through their pharmaceutical contamination (Yaoundé, Center Region, Cameroon). Sci. Total Environ. 660, 886–898. https://doi.org/https://doi.org/10.1016/j.scitotenv.2018.12.256

Buss, W., Graham, M.C., MacKinnon, G., Mašek, O., 2016. Strategies for producing biochars with minimum PAH contamination. J. Anal. Appl. Pyrolysis 119, 24–30. https://doi.org/https://doi.org/10.1016/j.jaap.2016.04.001

Buzgar, N., Ionut Apopei, A., 2009. The Raman study of Carbonates. Geologie 55, 97–112.

Chaukura, N., Murimba, E.C., Gwenzi, W., 2017. Sorptive removal of methylene blue from simulated wastewater using biochars derived from pulp and paper sludge. Environ. Technol. Innov. 8, 132–140. https://doi.org/https://doi.org/10.1016/j.eti.2017.06.004

Chen, X., Yang, L., Myneni, S.C.B., Deng, Y., 2019. Leaching of polycyclic aromatic hydrocarbons (PAHs) from sewage sludge-derived biochar. Chem. Eng. J. 373, 840–845. https://doi.org/https://doi.org/10.1016/j.cej.2019.05.059

Chowdhury, S., Mazumder, M.A.J., Al-Attas, O., Husain, T., 2016. Heavy metals in drinking water: Occurrences, implications, and future needs in developing countries. Sci. Total Environ. 569–570, 476–488. https://doi.org/https://doi.org/10.1016/j.scitotenv.2016.06.166

Czajczyńska, D., Anguilano, L., Ghazal, H., Krzyżyńska, R., Reynolds, A.J., Spencer, N., Jouhara, H., 2017. Potential of pyrolysis processes in the waste management sector. Therm. Sci. Eng. Prog. 3, 171–197. https://doi.org/https://doi.org/10.1016/j.tsep.2017.06.003

Devi, P., Saroha, A.K., 2013. Effect of temperature on biochar properties during paper. Int. Conf. Glob. Scenar. Environ. Energy.

Fan, Q., Sun, J., Chu, L., Cui, L., Quan, G., Yan, J., Hussain, Q., Iqbal, M., 2018. Effects of chemical oxidation on surface oxygen-containing functional groups and adsorption behavior of biochar. Chemosphere 207, 33–40. https://doi.org/https://doi.org/10.1016/j.chemosphere.2018.05.044

Fan, S., Tang, Jie, Wang, Y., Li, H., Zhang, H., Tang, Jun, Wang, Z., Li, X., 2016. Biochar prepared from co-pyrolysis of municipal sewage sludge and tea waste for the adsorption of methylene blue from aqueous solutions: Kinetics, isotherm, thermodynamic and mechanism. J. Mol. Liq. 220, 432–441. https://doi.org/https://doi.org/10.1016/j.molliq.2016.04.107

Fan, S., Wang, Y., Wang, Z., Tang, Jie, Tang, Jun, Li, X., 2017. Removal of methylene blue from aqueous solution by sewage sludge-derived biochar: Adsorption kinetics, equilibrium, thermodynamics and mechanism. J. Environ. Chem. Eng. 5, 601–611. https://doi.org/https://doi.org/10.1016/j.jece.2016.12.019

Farges, R., Gharzouni, A., Ravier, B., Jeulin, P., Rossignol, S., 2018. Insulating foams and dense geopolymers from biochar by-products. J. Ceram. Sci. Technol. 9, 193–200. https://doi.org/10.4416/JCST2017-00098

Fuertes, A.B., Arbestain, M.C., Sevilla, M., MacIá-Agulló, J.A., Fiol, S., López, R., Smernik, R.J., Aitkenhead, W.P., Arce, F., MacIas, F., 2010. Chemical and structural properties of carbonaceous products obtained by pyrolysis and hydrothermal carbonisation of corn stover. Aust. J. Soil Res. 48, 618–626. https://doi.org/10.1071/SR10010

Graf, N., Battes, K.P., Cimpean, M., Dittrich, P., Entling, M.H., Link, M., Scharmüller, A., Schreiner, V.C., Szöcs, E., Schäfer, R.B., 2019. Do agricultural pesticides in streams influence riparian spiders? Sci. Total Environ. 660, 126–135. https://doi.org/https://doi.org/10.1016/j.scitotenv.2018.12.370

Gundupalli, S.P., Hait, S., Thakur, A., 2017. A review on automated sorting of source-separated municipal solid waste for recycling. Waste Manag. 60, 56–74. https://doi.org/https://doi.org/10.1016/j.wasman.2016.09.015

Gwenzi, W., Chaukura, N., Mukome, F.N.D., Machado, S., Nyamasoka, B., 2015. Biochar production and applications in sub-Saharan Africa: Opportunities, constraints, risks and uncertainties. J. Environ. Manage. 150, 250–261. https://doi.org/https://doi.org/10.1016/j.jenvman.2014.11.027

Gwenzi, W., Chaukura, N., Noubactep, C., Mukome, F.N.D., 2017. Biochar-based water treatment systems as a potential low-cost and sustainable technology for clean water provision. J. Environ. Manage. 197, 732–749. https://doi.org/https://doi.org/10.1016/j.jenvman.2017.03.087

Hale, S.E., Lehmann, J., Rutherford, D., Zimmerman, A.R., Bachmann, R.T., Shitumbanuma, V., O'Toole, A., Sundqvist, K.L., Arp, H.P.H., Cornelissen, G., 2012. Quantifying the Total and Bioavailable Polycyclic Aromatic Hydrocarbons and Dioxins in Biochars. Environ. Sci. Technol. 46, 2830–2838. https://doi.org/10.1021/es203984k

He, J., Cui, A., Deng, S., Chen, J.P., 2018. Treatment of methylene blue containing wastewater by a cost-effective micro-scale biochar/polysulfone mixed matrix hollow fiber membrane: Performance and mechanism studies. J. Colloid Interface Sci. 512, 190–197. https://doi.org/https://doi.org/10.1016/j.jcis.2017.09.106

Hoslett, J., Ghazal, H., Ahmad, D., Jouhara, H., 2019. Removal of copper ions from aqueous solution using low temperature biochar derived from the pyrolysis of municipal solid waste. Sci. Total Environ. 673, 777–789. https://doi.org/10.1016/j.scitotenv.2019.04.085

Hoslett, J., Massara, T.M., Malamis, S., Ahmad, D., van den Boogaert, I., Katsou, E., Ahmad, B., Ghazal, H., Simons, S., Wrobel, L., Jouhara, H., 2018. Surface water filtration using granular media and membranes: A review. Sci. Total Environ. 639, 1268–1282. https://doi.org/https://doi.org/10.1016/j.scitotenv.2018.05.247

Hu, Y., Yu, W., Wibowo, H., Xia, Y., Lu, Y., Yan, M., 2019. Effect of catalysts on distribution of

polycyclic-aromatic hydrocarbon (PAHs) in bio-oils from the pyrolysis of dewatered sewage sludge at high and low temperatures. Sci. Total Environ. 667, 263–270. https://doi.org/https://doi.org/10.1016/j.scitotenv.2019.02.320

Huang, H., Buekens, A., 1995. On the mechanisms of dioxin formation in combustion processes. Chemosphere 31, 4099–4117. https://doi.org/https://doi.org/10.1016/0045-6535(95)80011-9

Huang, Y.-H., Liu, Y., Du, P.-P., Zeng, L.-J., Mo, C.-H., Li, Y.-W., Lü, H., Cai, Q.-Y., 2019. Occurrence and distribution of antibiotics and antibiotic resistant genes in water and sediments of urban rivers with black-odor water in Guangzhou, South China. Sci. Total Environ. 670, 170–180. https://doi.org/https://doi.org/10.1016/j.scitotenv.2019.03.168

Ibn Ferjani, A., Jeguirim, M., Jellali, S., Limousy, L., Courson, C., Akrout, H., Thevenin, N., Ruidavets, L., Muller, A., Bennici, S., 2019. The use of exhausted grape marc to produce biofuels and biofertilizers: Effect of pyrolysis temperatures on biochars properties. Renew. Sustain. Energy Rev. 107, 425–433. https://doi.org/https://doi.org/10.1016/j.rser.2019.03.034

Jouhara, H., Ahmad, D., Czajczyńska, D., Ghazal, H., Anguilano, L., Reynolds, A., Rutkowski, P., Krzyżyńska, R., Katsou, E., Simons, S., Spencer, N., 2018. Experimental investigation on the chemical characterisation of pyrolytic products of discarded food at temperatures up to 300 °C. Therm. Sci. Eng. Prog. 5, 579–588. https://doi.org/https://doi.org/10.1016/j.tsep.2018.02.010

Jouhara, H., Czajczyńska, D., Ghazal, H., Krzyżyńska, R., Anguilano, L., Reynolds, A.J., Spencer, N., 2017. Municipal waste management systems for domestic use. Energy 139, 485–506. https://doi.org/https://doi.org/10.1016/j.energy.2017.07.162

Kaza, S., Yao, L., Bhada-Tata, P., Van Woerden, F., 2018. What a Waste 2.0: A Global Snapshot of Solid Waste Management to 2050. The World Bank, Washington D.C. https://doi.org/10.1596/978-1-4648-1329-0

Lee, E., Oki, L.R., 2013. Slow sand filters effectively reduce Phytophthora after a pathogen switch from Fusarium and a simulated pump failure. Water Res. 47, 5121–5129. https://doi.org/https://doi.org/10.1016/j.watres.2013.05.054

Lee, H., Im, S.-J., Park, J.H., Jang, A., 2019. Removal and transport behavior of trace organic compounds and degradation byproducts in forward osmosis process: Effects of operation conditions and membrane properties. Chem. Eng. J. 375, 122030.

https://doi.org/https://doi.org/10.1016/j.cej.2019.122030

Li, L., Zou, D., Xiao, Z., Zeng, X., Zhang, L., Jiang, L., Wang, A., Ge, D., Zhang, G., Liu, F., 2019. Biochar as a sorbent for emerging contaminants enables improvements in waste management and sustainable resource use. J. Clean. Prod. 210, 1324–1342. https://doi.org/https://doi.org/10.1016/j.jclepro.2018.11.087

Li, S., Harris, S., Anandhi, A., Chen, G., 2019. Predicting biochar properties and functions based on feedstock and pyrolysis temperature: A review and data syntheses. J. Clean. Prod. 215, 890–902. https://doi.org/https://doi.org/10.1016/j.jclepro.2019.01.106

Li, S., Sanna, A., Andresen, J.M., 2011. Influence of temperature on pyrolysis of recycled organic matter from municipal solid waste using an activated olivine fluidized bed. Fuel Process. Technol. 92, 1776–1782. https://doi.org/https://doi.org/10.1016/j.fuproc.2011.04.026

Litescu, S.C., Teodor, E.D., Truica, G., Tache, A., Radu, G., 2012. Fourier Transform Infrared Spectroscopy - Useful Analytical Tool for Non-Destructive Analysis. https://doi.org/10.5772/36428

Liu, J., Zhou, B., Zhang, H., Ma, J., Mu, B., Zhang, W., 2019. A novel Biochar modified by Chitosan-Fe/S for tetracycline adsorption and studies on site energy distribution. Bioresour. Technol. 294, 122152. https://doi.org/https://doi.org/10.1016/j.biortech.2019.122152

Liu, S., Li, J., Xu, S., Wang, M., Zhang, Y., Xue, X., 2019. A Modified Method for Enhancing Adsorption Capability of Banana Pseudostem Biochar towards Methylene Blue at Low Temperature. Bioresour. Technol. https://doi.org/https://doi.org/10.1016/j.biortech.2019.02.092

Lonappan, L., Rouissi, T., Das, R.K., Brar, S.K., Ramirez, A.A., Verma, M., Surampalli, R.Y., Valero, J.R., 2016. Adsorption of methylene blue on biochar microparticles derived from different waste materials. Waste Manag. 49, 537–544. https://doi.org/https://doi.org/10.1016/j.wasman.2016.01.015

Lyu, H., Gao, B., He, F., Zimmerman, A.R., Ding, C., Tang, J., Crittenden, J.C., 2018. Experimental and modeling investigations of ball-milled biochar for the removal of aqueous methylene blue. Chem. Eng. J. 335, 110–119. https://doi.org/https://doi.org/10.1016/j.cej.2017.10.130

Mac Mahon, J., Gill, L.W., 2018. Sustainability of novel water treatment technologies in

developing countries: Lessons learned from research trials on a pilot continuous flow solar water disinfection system in rural Kenya. Dev. Eng. 3, 47–59. https://doi.org/https://doi.org/10.1016/j.deveng.2018.01.003

Manawi, Y., McKay, G., Ismail, N., Kayvani Fard, A., Kochkodan, V., Atieh, M.A., 2018. Enhancing lead removal from water by complex-assisted filtration with acacia gum. Chem. Eng. J. 352, 828–836. https://doi.org/https://doi.org/10.1016/j.cej.2018.07.087

Meira de Sousa Dutra, R., Harue Yamane, L., Ribeiro Siman, R., 2018. Influence of the expansion of the selective collection in the sorting infrastructure of waste pickers' organizations: A case study of 16 Brazilian cities. Waste Manag. 77, 50–58. https://doi.org/https://doi.org/10.1016/j.wasman.2018.05.009

Minomo, K., Ohtsuka, N., Nojiri, K., Matsumoto, R., 2018. Influence of combustion-originated dioxins in atmospheric deposition on water quality of an urban river in Japan. J. Environ. Sci. 64, 245–251. https://doi.org/https://doi.org/10.1016/j.jes.2017.06.027

Mohammed, N.A.S., Abu-Zurayk, R.A., Hamadneh, I., Al-Dujaili, A.H., 2018. Phenol adsorption on biochar prepared from the pine fruit shells: Equilibrium, kinetic and thermodynamics studies. J. Environ. Manage. 226, 377–385. https://doi.org/https://doi.org/10.1016/j.jenvman.2018.08.033

Molina Higgins, M., Toro González, M., Rojas, J., 2019. Enhanced X-RAYS degradation of methylene blue in the presence of gold microspheres. Radiat. Phys. Chem. 156, 73–80. https://doi.org/https://doi.org/10.1016/j.radphyschem.2018.10.020

Parsa, M., Nourani, M., Baghdadi, M., Hosseinzadeh, M., Pejman, M., 2019. Biochars derived from marine macroalgae as a mesoporous by-product of hydrothermal liquefaction process: Characterization and application in wastewater treatment. J. Water Process Eng. 32, 100942. https://doi.org/https://doi.org/10.1016/j.jwpe.2019.100942

Paunovic, O., Pap, S., Maletic, S., Taggart, M.A., Boskovic, N., Turk Sekulic, M., 2019. Ionisable emerging pharmaceutical adsorption onto microwave functionalised biochar derived from novel lignocellulosic waste biomass. J. Colloid Interface Sci. 547, 350–360. https://doi.org/https://doi.org/10.1016/j.jcis.2019.04.011

Petrovic, M., Sremacki, M., Radonic, J., Mihajlovic, I., Obrovski, B., Vojinovic Miloradov, M., 2018. Health risk assessment of PAHs, PCBs and OCPs in atmospheric air of municipal solid waste landfill in Novi Sad, Serbia. Sci. Total Environ. 644, 1201–1206. https://doi.org/https://doi.org/10.1016/j.scitotenv.2018.07.008

Que, W., Jiang, L., Wang, C., Liu, Y., Zeng, Z., Wang, X., Ning, Q., Liu, Shaoheng, Zhang, P., Liu, Shaobo, 2018. Influence of sodium dodecyl sulfate coating on adsorption of methylene blue by biochar from aqueous solution. J. Environ. Sci. 70, 166–174. https://doi.org/https://doi.org/10.1016/j.jes.2017.11.027

Quesada, H.B., Baptista, A.T.A., Cusioli, L.F., Seibert, D., de Oliveira Bezerra, C., Bergamasco, R., 2019. Surface water pollution by pharmaceuticals and an alternative of removal by low-cost adsorbents: A review. Chemosphere 222, 766–780. https://doi.org/https://doi.org/10.1016/j.chemosphere.2019.02.009

Rajapaksha, A.U., Ok, Y.S., El-Naggar, A., Kim, H., Song, F., Kang, S., Tsang, Y.F., 2019. Dissolved organic matter characterization of biochars produced from different feedstock materials. J. Environ. Manage. 233, 393–399. https://doi.org/https://doi.org/10.1016/j.jenvman.2018.12.069

Rashid, J., Tehreem, F., Rehman, A., Kumar, R., 2019. Synthesis using natural functionalization of activated carbon from pumpkin peels for decolourization of aqueous methylene blue. Sci. Total Environ. 671, 369–376. https://doi.org/https://doi.org/10.1016/j.scitotenv.2019.03.363

Rechberger, M. V, Kloss, S., Wang, S.-L., Lehmann, J., Rennhofer, H., Ottner, F., Wriessnig, K., Daudin, G., Lichtenegger, H., Soja, G., Zehetner, F., 2019. Enhanced Cu and Cd sorption after soil aging of woodchip-derived biochar: What were the driving factors? Chemosphere 216, 463–471. https://doi.org/https://doi.org/10.1016/j.chemosphere.2018.10.094

Rehman, S., Adil, A., Shaikh, A.J., Shah, J.A., Arshad, M., Ali, M.A., Bilal, M., 2018. Role of sorption energy and chemisorption in batch methylene blue and Cu2+ adsorption by novel thuja cone carbon in binary component system: linear and nonlinear modeling. Environ. Sci. Pollut. Res. 25, 31579–31592. https://doi.org/10.1007/s11356-018-2958-2

Ren, X., Wang, F., Zhang, P., Guo, J., Sun, H., 2018. Aging effect of minerals on biochar properties and sorption capacities for atrazine and phenanthrene. Chemosphere 206, 51–58. https://doi.org/https://doi.org/10.1016/j.chemosphere.2018.04.125

Sanganyado, E., Gwenzi, W., 2019. Antibiotic resistance in drinking water systems: Occurrence, removal, and human health risks. Sci. Total Environ. 669, 785–797. https://doi.org/https://doi.org/10.1016/j.scitotenv.2019.03.162

Sasidharan, S., Torkzaban, S., Bradford, S.A., Kookana, R., Page, D., Cook, P.G., 2016. Transport

and retention of bacteria and viruses in biochar-amended sand. Sci. Total Environ. 548–549, 100–109. https://doi.org/https://doi.org/10.1016/j.scitotenv.2015.12.126

Schreiter, I.J., Schmidt, W., Schüth, C., 2018. Sorption mechanisms of chlorinated hydrocarbons on biochar produced from different feedstocks: Conclusions from single- and bi-solute experiments. Chemosphere 203, 34–43. https://doi.org/https://doi.org/10.1016/j.chemosphere.2018.03.173

Seo, Y.B., Ahn, J.H., Lee, H.L., 2017. Upgrading waste paper by in-situ calcium carbonate formation. J. Clean. Prod. 155, 212–217. https://doi.org/https://doi.org/10.1016/j.jclepro.2016.09.003

Sheng, C., 2007. Char structure characterised by Raman spectroscopy and its correlations with combustion reactivity. Fuel 86, 2316–2324. https://doi.org/10.1016/j.fuel.2007.01.029

Shooto, N.D., Nkutha, C.S., Guilande, N.R., Naidoo, E.B., 2020. Pristine and modified mucuna beans adsorptive studies of toxic lead ions and methylene blue dye from aqueous solution. South African J. Chem. Eng. 31, 33–43. https://doi.org/https://doi.org/10.1016/j.sajce.2019.12.001

Singh, R., Singh, A.P., Kumar, S., Giri, B.S., Kim, K.-H., 2019. Antibiotic Resistance in Major Rivers in the World: A Systematic Review on Occurrence, Emergence, and Management Strategies. J. Clean. Prod. https://doi.org/https://doi.org/10.1016/j.jclepro.2019.06.243

Sophonrat, N., Sandström, L., Zaini, I.N., Yang, W., 2018. Stepwise pyrolysis of mixed plastics and paper for separation of oxygenated and hydrocarbon condensates. Appl. Energy 229, 314–325. https://doi.org/https://doi.org/10.1016/j.apenergy.2018.08.006

Sumalinog, D.A.G., Capareda, S.C., de Luna, M.D.G., 2018. Evaluation of the effectiveness and mechanisms of acetaminophen and methylene blue dye adsorption on activated biochar derived from municipal solid wastes. J. Environ. Manage. 210, 255–262. https://doi.org/https://doi.org/10.1016/j.jenvman.2018.01.010

Sun, C., Chen, L., Zhai, L., Liu, H., Jiang, Y., Wang, K., Jiao, C., Shen, Z., 2019. National assessment of spatiotemporal loss in agricultural pesticides and related potential exposure risks to water quality in China. Sci. Total Environ. 677, 98–107. https://doi.org/https://doi.org/10.1016/j.scitotenv.2019.04.346

Sun, L., Wan, S., Luo, W., 2013. Biochars prepared from anaerobic digestion residue, palm bark, and eucalyptus for adsorption of cationic methylene blue dye: Characterization, equilibrium, and kinetic studies. Bioresour. Technol. 140, 406–413.

https://doi.org/https://doi.org/10.1016/j.biortech.2013.04.116

Suo, F., You, X., Ma, Y., Li, Y., 2019. Rapid removal of triazine pesticides by P doped biochar and the adsorption mechanism. Chemosphere 235, 918–925. https://doi.org/https://doi.org/10.1016/j.chemosphere.2019.06.158

Tan, Z., Yuan, S., Hong, M., Zhang, L., Huang, Q., 2019. Mechanism of Negative Surface Charge Formation on Biochar and its Effect on the Fixation of Soil Cd. J. Hazard. Mater. 121370. https://doi.org/https://doi.org/10.1016/j.jhazmat.2019.121370

Tang, Y., Alam, M.S., Konhauser, K.O., Alessi, D.S., Xu, S., Tian, W., Liu, Y., 2019. Influence of pyrolysis temperature on production of digested sludge biochar and its application for ammonium removal from municipal wastewater. J. Clean. Prod. 209, 927–936. https://doi.org/https://doi.org/10.1016/j.jclepro.2018.10.268

Tizaoui, C., Rachmawati, S.D., Hilal, N., 2012. The removal of copper in water using manganese activated saturated and unsaturated sand filters. Chem. Eng. J. 209, 334–344. https://doi.org/https://doi.org/10.1016/j.cej.2012.08.013

Tong, D.S., Wu, C.W., Adebajo, M.O., Jin, G.C., Yu, W.H., Ji, S.F., Zhou, C.H., 2018. Adsorption of methylene blue from aqueous solution onto porous cellulose-derived carbon/montmorillonite nanocomposites. Appl. Clay Sci. 161, 256–264. https://doi.org/https://doi.org/10.1016/j.clay.2018.02.017

Trakal, L., Veselská, V., Šafařík, I., Vítková, M., Číhalová, S., Komárek, M., 2016. Lead and cadmium sorption mechanisms on magnetically modified biochars. Bioresour. Technol. 203, 318–324. https://doi.org/https://doi.org/10.1016/j.biortech.2015.12.056

US, N. (National I. of E.H.S., 2019. Endocrine Disruptors [WWW Document]. URL https://www.niehs.nih.gov/health/topics/agents/endocrine/index.cfm (accessed 8.22.19).

Van Poucke, R., Allaert, S., Ok, Y.S., Pala, M., Ronsse, F., Tack, F.M.G., Meers, E., 2019. Metal sorption by biochars: A trade-off between phosphate and carbonate concentration as governed by pyrolysis conditions. J. Environ. Manage. 246, 496–504. https://doi.org/https://doi.org/10.1016/j.jenvman.2019.05.112

Vandermarken, T., Gao, Y., Baeyens, W., Denison, M.S., Croes, K., 2018. Dioxins, furans and dioxin-like PCBs in sediment samples and suspended particulate matter from the Scheldt estuary and the North Sea Coast: Comparison of CALUX concentration levels in historical and recent samples. Sci. Total Environ. 626, 109–116.

https://doi.org/https://doi.org/10.1016/j.scitotenv.2018.01.084

Wang, Y., Zhang, Y., Li, S., Zhong, W., Wei, W., 2018. Enhanced methylene blue adsorption onto activated reed-derived biochar by tannic acid. J. Mol. Liq. 268, 658–666. https://doi.org/https://doi.org/10.1016/j.molliq.2018.07.085

Wei, J., Tu, C., Yuan, G., Liu, Y., Bi, D., Xiao, L., Lu, J., Theng, B.K.G., Wang, H., Zhang, L., Zhang, X., 2019. Assessing the effect of pyrolysis temperature on the molecular properties and copper sorption capacity of a halophyte biochar. Environ. Pollut. 251, 56–65. https://doi.org/https://doi.org/10.1016/j.envpol.2019.04.128

Wongrod, S., Simon, S., van Hullebusch, E.D., Lens, P.N.L., Guibaud, G., 2019. Assessing arsenic redox state evolution in solution and solid phase during As(III) sorption onto chemically-treated sewage sludge digestate biochars. Bioresour. Technol. 275, 232–238. https://doi.org/https://doi.org/10.1016/j.biortech.2018.12.056

Yaashikaa, P.R., Senthil Kumar, P., Varjani, S.J., Saravanan, A., 2019. Advances in production and application of biochar from lignocellulosic feedstocks for remediation of environmental pollutants. Bioresour. Technol. 292, 122030. https://doi.org/https://doi.org/10.1016/j.biortech.2019.122030

Yang, Y., Heaven, S., Venetsaneas, N., Banks, C.J., Bridgwater, A. V, 2018. Slow pyrolysis of organic fraction of municipal solid waste (OFMSW): Characterisation of products and screening of the aqueous liquid product for anaerobic digestion. Appl. Energy 213, 158–168. https://doi.org/https://doi.org/10.1016/j.apenergy.2018.01.018

Yazdani, M.R., Duimovich, N., Tiraferri, A., Laurell, P., Borghei, M., Zimmerman, J.B., Vahala, R., 2019. Tailored mesoporous biochar sorbents from pinecone biomass for the adsorption of natural organic matter from lake water. J. Mol. Liq. 291, 111248. https://doi.org/https://doi.org/10.1016/j.molliq.2019.111248

Yuan, P., Wang, J., Pan, Y., Shen, B., Wu, C., 2019. Review of biochar for the management of contaminated soil: Preparation, application and prospect. Sci. Total Environ. 659, 473–490. https://doi.org/https://doi.org/10.1016/j.scitotenv.2018.12.400

Zhang, P., O'Connor, D., Wang, Y., Jiang, L., Xia, T., Wang, L., Tsang, D.C.W., Ok, Y.S., Hou, D., 2020. A green biochar/iron oxide composite for methylene blue removal. J. Hazard. Mater. 384, 121286. https://doi.org/https://doi.org/10.1016/j.jhazmat.2019.121286

Zhang, Q., Saleem, M., Wang, C., 2019. Effects of biochar on the earthworm (Eisenia foetida) in soil contaminated with and/or without pesticide mesotrione. Sci. Total Environ. 671,

52–58. https://doi.org/https://doi.org/10.1016/j.scitotenv.2019.03.364

Zhang, X., Gao, B., Zheng, Y., Hu, X., Creamer, A.E., Annable, M.D., Li, Y., 2017. Biochar for volatile organic compound (VOC) removal: Sorption performance and governing mechanisms. Bioresour. Technol. 245, 606–614. https://doi.org/https://doi.org/10.1016/j.biortech.2017.09.025

Zhao, Z., Nie, T., Zhou, W., 2019. Enhanced biochar stabilities and adsorption properties for tetracycline by synthesizing silica-composited biochar. Environ. Pollut. 254, 113015. https://doi.org/https://doi.org/10.1016/j.envpol.2019.113015

Zhou, H., Wu, C., Onwudili, J.A., Meng, A., Zhang, Y., Williams, P.T., 2016. Influence of process conditions on the formation of 2–4 ring polycyclic aromatic hydrocarbons from the pyrolysis of polyvinyl chloride. Fuel Process. Technol. 144, 299–304. https://doi.org/https://doi.org/10.1016/j.fuproc.2016.01.013

Zhou, H., Wu, C., Onwudili, J.A., Meng, A., Zhang, Y., Williams, P.T., 2015. Polycyclic aromatic hydrocarbons (PAH) formation from the pyrolysis of different municipal solid waste fractions. Waste Manag. 36, 136–146. https://doi.org/https://doi.org/10.1016/j.wasman.2014.09.014

Zhu, Y., Yi, B., Yuan, Q., Wu, Y., Wang, M., Yan, S., 2018. Removal of methylene blue from aqueous solution by cattle manure-derived low temperature biochar. RSC Adv. 8, 19917–19929. https://doi.org/10.1039/C8RA03018A